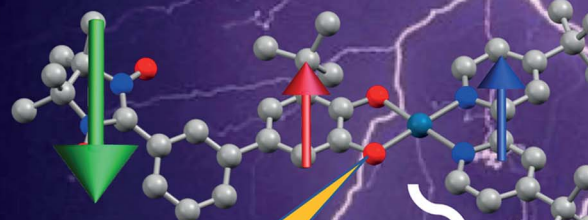
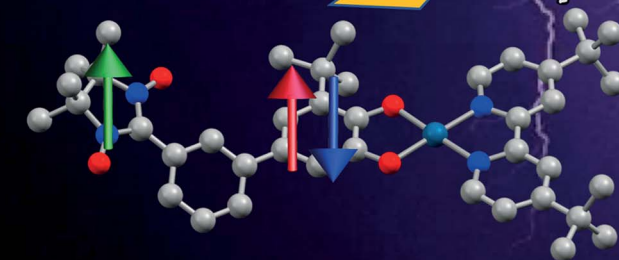


## Entangled 3-Spin Excited State



## Light-Induced Ground State Electron Spin Polarization

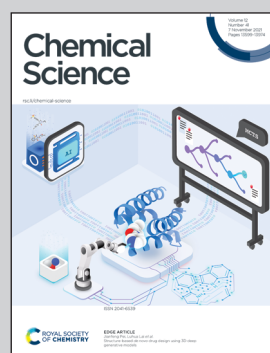


Showcasing research from Professor Martin L. Kirk's laboratory, Department of Chemistry and Chemical Biology, The University of New Mexico, Albuquerque, NM, USA, and Professor David A. Shultz's laboratory, Department of Chemistry, North Carolina State University, Raleigh, NC, USA.

Chromophore-radical excited state antiferromagnetic exchange controls the sign of photoinduced ground state spin polarization

We observe dramatic differences in ground state electron spin polarization (ESP) as a function of the antiferromagnetic chromophore-radical exchange interaction in radical elaborated donor-acceptor complexes. Specifically, small conformational changes along low-frequency torsional modes of these radical-donor-acceptor molecules result in conformational exchange modulation that affects the sign and magnitude of the ground state ESP. The work highlights the importance of subtle changes in excited state electronic structure, and how this affects excited state properties and dynamics that control ESP relevant to quantum information science applications.

### As featured in:



See Martin L. Kirk, David A. Shultz, Art van der Est *et al.*, *Chem. Sci.*, 2021, **12**, 13704.



Cite this: *Chem. Sci.*, 2021, **12**, 13704

All publication charges for this article have been paid for by the Royal Society of Chemistry

## Chromophore-radical excited state antiferromagnetic exchange controls the sign of photoinduced ground state spin polarization†

Martin L. Kirk, <sup>†,\*a</sup> David A. Shultz, <sup>†,\*b</sup> Patrick Hewitt, <sup>b</sup> Daniel E. Stasiw, <sup>b</sup> Ju Chen <sup>a</sup> and Art van der Est <sup>†,\*c</sup>

A change in the sign of the ground-state electron spin polarization (ESP) is reported in complexes where an organic radical (nitronylnitroxide, NN) is covalently attached to a donor–acceptor chromophore via two different *meta*-phenylene bridges in (bpy)Pt(CAT-*m*-Ph-NN) (*m*Ph-Pt) and (bpy)Pt(CAT-6-Me-*m*-Ph-NN) (6-Me-*m*Ph-Pt) (bpy = 5,5'-di-*tert*-butyl-2,2'-bipyridine, CAT = 3-*tert*-butylcatecholate, *m*-Ph = *meta*-phenylene). These molecules represent a new class of chromophores that can be photoexcited with visible light to produce an initial exchange-coupled, 3-spin (bpy<sup>+</sup>, CAT<sup>+</sup> = semiquinone (SQ), and NN), charge-separated doublet <sup>2</sup>S<sub>1</sub> (S = chromophore excited spin singlet configuration) excited state. Following excitation, the <sup>2</sup>S<sub>1</sub> state rapidly decays to the ground state by magnetic exchange-mediated enhanced internal conversion via the <sup>2</sup>T<sub>1</sub> (T = chromophore excited spin triplet configuration) state. This process generates emissive ground state ESP in 6-Me-*m*Ph-Pt while for *m*Ph-Pt the ESP is absorptive. It is proposed that the emissive polarization in 6-Me-*m*Ph-Pt results from zero-field splitting induced transitions between the chromophoric <sup>2</sup>T<sub>1</sub> and <sup>4</sup>T<sub>1</sub> states, whereas predominant spin–orbit induced transitions between <sup>2</sup>T<sub>1</sub> and low-energy NN-based states give rise to the absorptive polarization observed for *m*Ph-Pt. The difference in the sign of the ESP for these molecules is consistent with a smaller excited state <sup>2</sup>T<sub>1</sub> – <sup>4</sup>T<sub>1</sub> gap for 6-Me-*m*Ph-Pt that derives from steric interactions with the 6-methyl group. These steric interactions reduce the excited state pairwise SQ-NN exchange coupling compared to that in *m*Ph-Pt.

Received 2nd June 2021

Accepted 1st September 2021

DOI: 10.1039/d1sc02965g

rsc.li/chemical-science

## Introduction

Molecular quantum information science (QIS) requires the synthesis and study of new molecules that can enable the generation, manipulation, and readout of specifically prepared quantum states<sup>1</sup> in order to advance new nanoscale technologies that include, computing,<sup>2–5</sup> sensing,<sup>6,7</sup> and communications.<sup>8</sup> QIS exploits quantum bits, or qubits, that are unlike two-level classical bits (e.g., binary 0 and 1) since they can be entangled and exist as superposition states described by linear

combinations of these 0 and 1 binary representations.<sup>1,9</sup> An unpaired electron spin ( $S = 1/2$ ,  $m_s \pm 1/2$ ) represents such a two-level quantum system that can be created with relative ease in a molecular environment. However, expanding such a system to include multiple unpaired spins and generating the desired coherences within the system represents a significant challenge.

Building on our earlier work,<sup>10–16</sup> we have shown that photoexcitation into the low-energy ligand-to-ligand charge transfer (LL/CT) bands of bipyridine-metal-catecholate ((bpy)M(CAT)) complexes with M = Pt or Pd provide a convenient way to generate charge transfer excited states with considerable biradical spin character.<sup>11–13,16,17</sup> When these molecules are elaborated with a persistent radical attached to the CAT donor, the LL/CT excited states can be described as having three localized spin qubits that possess different pairwise exchange interactions.<sup>16,17</sup> A particular benefit of this tripartite entanglement<sup>9,18–20</sup> is that when the spins in the open-shell excited singlet- (S) and triplet (T) states of the chromophore exchange couple with the radical, two doublet states (<sup>2</sup>S<sub>1</sub> and <sup>2</sup>T<sub>1</sub>) and a quartet state (<sup>4</sup>T<sub>1</sub>) result, and magnetic exchange interactions admix the <sup>2</sup>S<sub>1</sub> and <sup>2</sup>T<sub>1</sub> states.<sup>17</sup> This excited state exchange mixing effectively mediates an enhanced inter-system crossing<sup>21–24</sup> that permits access to the localized high-spin triplet configuration of the chromophore. The triplet state of the (bpy)M(CAT) parent chromophore is otherwise inaccessible due to

<sup>a</sup>Department of Chemistry and Chemical Biology, The University of New Mexico, MSC03 2060, 1 University of New Mexico, Albuquerque, NM 87131-0001, USA. E-mail: mkirk@unm.edu

<sup>b</sup>Department of Chemistry, North Carolina State University, Raleigh, North Carolina 27695-8204, USA. E-mail: shultz@ncsu.edu

<sup>c</sup>Department of Chemistry, Brock University, St. Catharines, Ontario, Canada L2S 3A1. E-mail: avanderest@brocku.ca

† Electronic supplementary information (ESI) available: Synthesis and characterization of 6-Me-*m*Ph-Pt and related complexes, X-ray crystallographic analysis for LZN(SQ-6-Me-*m*Ph-NN). CCDC 2087657. For ESI and crystallographic data in CIF or other electronic format see DOI: 10.1039/d1sc02965g

‡ These authors contributed equally.

§ Present address: Cree, RTP, Durham, NC.



non-competitive intersystem crossing (ISC) rates compared to efficient non-radiative relaxation back to the singlet ground state.<sup>13,15</sup>

Chromophores with appended radicals have been used to provide high-resolution information regarding the nature of their low-energy excited states,<sup>11,12,16,17</sup> illustrate how multiple, pairwise, excited state magnetic exchange interactions influence photophysical processes,<sup>11</sup> and highlight how the excited state chromophore triplet – radical magnetic exchange interaction and associated excited state dynamics can affect electron spin polarization (ESP).<sup>11,16,17,22,23,25–34</sup> In most systems of this type, ESP is a result of the spin selectivity of the transitions between nearly degenerate  $^2T_1$  and  $^4T_1$  states and, in the absence of intermolecular collisions, ESP is observed when these states are relatively long lived. These radical-elaborated chromophores possess spin-polarized quartet  $^4T_1$  excited states with lifetimes that compete with or exceed the spin-lattice relaxation time ( $T_1$ ) of the appended radical, and this effectively inhibits the transfer of ESP to the electronic ground state. Although the observation of ground state ESP is rare in glassy matrices, a few examples are known and they occur *via* the reversed quartet mechanism (RQM, Fig. 1).<sup>35,36</sup>

Electron spin polarization,<sup>23,37,38</sup> including that generated by RQM,<sup>35,36</sup> derives from non-Boltzmann  $m_s$  sublevel populations (Fig. 1) and can be detected using time resolved electron paramagnetic resonance (TREPR) spectroscopy as either an enhanced emissive (Fig. 1A) or absorptive (Fig. 1B) signal. An emissive TREPR signal *via* the RQM requires the  $^4T_1$  state to be *higher* in energy than  $^2T_1$  (and  $\Delta E_{D1Q} \sim k_B T$  where  $k_B$  is Boltzmann's constant and  $T$  is temperature). In this case, spin selective transitions ( $k_{QD/QD}$ , Fig. 1) between the  $^2T_1$  and  $^4T_1$  states result in an excess population of the higher energy  $m_s = +1/2$  sublevel of the doublet and enhanced *emissive* ESP. Conversely, an absorptive TREPR signal *via* the RQM (Fig. 1B) requires the  $^4T_1$  quartet state to be *lower* in energy than the  $^2T_1$  doublet (and  $\Delta E \sim k_B T$ ). Here, spin selective transitions ( $k_{QD/QD}$ , Fig. 1) between  $^2T_1$  and  $^4T_1$  result in an excess population of the

lower-energy  $m_s = -1/2$  level of the doublet and enhanced *absorptive* ESP. This photogenerated  $^2T_1$  ESP can then be transferred to the ground state if  $^2T_1 \rightarrow ^2S_0$  relaxation is faster than the  $T_1$  spin relaxation of the appended radical in the  $^2S_0$  state. A key point of the RQM is that the *sign* of the exchange parameter determines the relative energy ordering of the  $^2T_1$  and  $^4T_1$  states, and whether the observed ESP will be absorptive or emissive.<sup>35,36</sup> This mechanism predicts that antiferromagnetic chromophore-radical exchange ( $J_{CR} < 0$ ), with  $E(^2T_1) < E(^4T_1)$ , results in emissive ESP (Fig. 1A), while ferromagnetic chromophore-radical exchange ( $J_{CR} > 0$ ), with  $E(^4T_1) < E(^2T_1)$ , yields absorptive ESP (Fig. 1B).<sup>35,36</sup>

Recently, we demonstrated that despite the short  $^2T_1$  excited state lifetime and absence of intermolecular collisions, strong *ground state* ESP can be generated in (bpy)Pt(CAT-*m*-Ph-NN) (**mPh-Pt**, NN = nitronylnitroxide radical).<sup>16</sup> The intensity of the photoinduced ESP in **mPh-Pt** was also shown to be dramatically altered by changing the metal ion from Pt to Pd in what are otherwise identical complexes.<sup>16</sup> In the present work, we show that the nature of the ground state ESP is also related to the *magnitude* of the excited state chromophore-radical antiferromagnetic exchange ( $J_{SQ-NN}$  ( $= 2J_{CR}$ ) Fig. 2A), which can be controlled by tailored bond torsions that reduce  $\pi$ -system mediated superexchange coupling. Thus the sign of the photogenerated ESP is not determined by changing the *sign* of  $J_{SQ-NN}$ , as predicted by the RQM.<sup>35,36</sup> Here, changing the magnitude of the excited state exchange affects how the coupled chromophore-radical  $^4T_1$ – $^2T_1$  states interact with localized states of the radical (*e.g.*,  $D_{NN}$ ,  $Q_{NN}$ , *vide infra*), suggesting a new mechanism for modulating the sign of ground state ESP.

## (Bipyridine)Pt<sup>II</sup>(catecholate-bridge-radical) complexes

The (bpy)M(CAT-Ph-NN) chromophoric system (Fig. 2A and B)<sup>11,16,17</sup> offers a synthetically flexible platform to explore magnetic exchange contributions to both the sign and

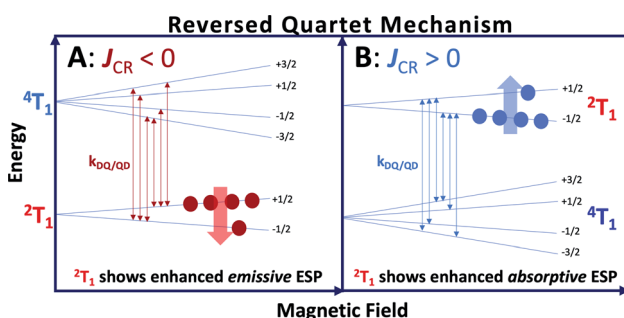


Fig. 1 Left (A): reversed quartet mechanism (RQM), antiferromagnetic  $J_{CR}$ . Spin-selective transitions ( $k_{QD/QD}$ ) between doublet and quartet result in non-Boltzmann population (red dots) of the doublet  $m_s$  levels (non-Boltzmann population of quartet not shown) resulting in enhanced emissive ESP. Right (B): RQM, ferromagnetic  $J_{CR}$ . Spin-selective transitions ( $k_{QD/QD}$ ) between doublet and quartet states result in non-Boltzmann population (blue dots) of the doublet  $m_s$  levels (non-Boltzmann population of quartet not shown) resulting in enhanced absorptive ESP.

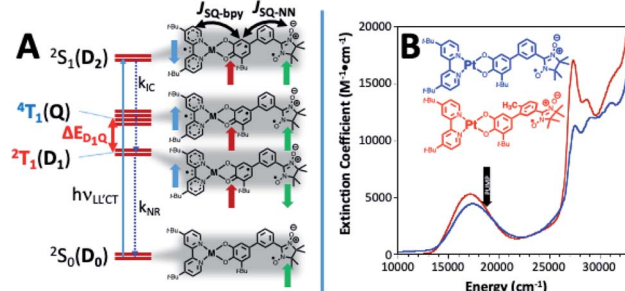


Fig. 2 (A) (Left) ground doublet- ( $^2S_0/D_0$ ) and LL'CT excited state manifold. Vertical doublet  $^2S_1(D_2)$  undergoes rapid internal conversion ( $k_{IC}$ ) to  $^2T_1(D_1)$ , which has (bpy)Pt(CAT) triplet character. Nonradiative decay of the  $^2T_1$  state ( $k_{NR}$ ) provides the  $^2S_0$  ground state with non-Boltzmann  $m_s$  populations. (Right) depictions of ground- ( $^2S_0/D_0$ ), and LL'CT excited states; magnetic exchange coupling parameters,  $J_{SQ-bpy}$  and  $J_{SQ-NN}$  defined;  $J_{SQ-NN}$  is related to  $J_{CR}$  in Fig. 1. (B) Electronic absorption spectra (300 K;  $CH_2Cl_2$ ), for **mPh-Pt** (blue line) and **6-Me-mPh-Pt** (red line), indicating TREPR photoexcitation energy relative to the  $\sim 17\ 000\ cm^{-1}$   $^2S_0(D_0) \rightarrow ^2S_1(D_2)$  LL'CT transition



magnitude of the photoinduced ground state ESP. Fig. 2B shows the virtually identical solution electronic absorption spectra of **mPh-Pt** and (bpy)Pt(CAT-6-Me-*m*-Ph-NN) (**6-Me-*m*-Ph-Pt**), where the characteristic low-energy CAT(HOMO)  $\rightarrow$  bpy(LUMO) ligand-to-ligand charge transfer (LL'CT) transitions are observed at  $\sim 17\,000\, \text{cm}^{-1}$ .<sup>11,15-17</sup> Interestingly, localized aryl-NN  $\pi \rightarrow \pi^*$  transitions are also observed in this spectral region,<sup>39,40</sup> but they are obscured in **mPh-Pt** and **6-Me-*m*-Ph-Pt** by the more intense LL'CT band.<sup>16</sup> Despite the remarkably similar electronic absorption spectra observed for (bpy)Pt(CAT-*bridge*-NN) complexes,<sup>17</sup> the nature of the magnetic exchange coupling between spins in the excited states of (bpy)Pt(CAT-*bridge*-NN) systems can dramatically affect excited state processes when compared to the parent (bpy)Pt(CAT) chromophore that lacks an appended radical.<sup>11</sup> This was previously exemplified by the observation of both magnetic circular dichroism (MCD) activity,<sup>17</sup> and a dramatic modulation of excited state lifetimes in (bpy)Pt(CAT-*bridge*-NN) molecules.<sup>11</sup>

Optical excitation into the **mPh-Pt** and **6-Me-*m*-Ph-Pt** spin-allowed  $^2\text{S}_0 \rightarrow ^2\text{S}_1$  LL'CT transition leads to a high degree of CAT  $\rightarrow$  bpy charge separation, and a bpy<sup>1</sup>CAT<sup>1</sup>NN<sup>1</sup> (*i.e.*, a bpy<sup>+</sup>SQ<sup>·</sup>NN<sup>·</sup> tri-radical; SQ = semiquinone; hereafter “” is omitted) electronic configuration that has  $^2\text{S}_1$ ,  $^2\text{T}_1$ , and  $^4\text{T}_1$  excited states (Fig. 2A and B).<sup>17</sup> The cross-conjugated *meta*-phenylene bridges in **mPh-Pt** and **6-Me-*m*-Ph-Pt** promote an antiferromagnetic chromophore – radical exchange interaction  $J_{\text{SQ-NN}}$ , Fig. 2A,<sup>41</sup> with the primary consequence being that the  $^2\text{T}_1$  state resides at lower energy than the high-spin  $^4\text{T}_1$  quartet excited state (Fig. 1A and 2A). Moreover, the spatial separation of the unpaired spins in the LL'CT state leads to large differences in the pairwise magnetic exchange couplings to the NN radical, which results in mixing of the  $^2\text{S}_1$  and  $^2\text{T}_1$  states, and ultrafast enhanced intersystem crossing (EISC)<sup>21,22,24</sup> from the  $^2\text{S}_1$  to the  $^2\text{T}_1$  state. Thus, photoexcitation followed by EISC ( $k_{\text{IC}}$ , Fig. 2A) results in  $^2\text{S}_0 \rightarrow ^2\text{S}_1 \rightarrow ^2\text{T}_1$  (Fig. 2A) for both **mPh-Pt** and **6-Me-*m*-Ph-Pt**. Fast non-radiative decay ( $k_{\text{NR}}$ , Fig. 2A) of the  $^2\text{T}_1$  state yields the  $^2\text{S}_0$  ground state.<sup>11,16,17</sup>

## The effect of bond torsions on excited state exchange

The key structural difference between **mPh-Pt** and **6-Me-*m*-Ph-Pt** is a single methyl substituent on the *meta*-phenylene bridge fragment of **6-Me-*m*-Ph-Pt** that results in increased CAT-bridge bond torsion. As seen in Fig. 2B, the CAT-bridge bond torsion results in modest changes in the LL'CT band by attenuating CAT-bridge delocalization.<sup>10</sup> The increased CAT-bridge torsion reduces the LL'CT excited state SQ-*m*Ph-NN  $\pi$ -overlap relative to that of **mPh-Pt**.<sup>10,14</sup> This reduction in  $\pi$ -overlap decreases the magnitude of  $J_{\text{SQ-NN}}$  in the LL'CT excited state of **6-Me-*m*-Ph-Pt** so that  $\Delta E_{\text{D1Q}}(\mathbf{6-Me-*m*-Ph-Pt}) < \Delta E_{\text{D1Q}}(\mathbf{mPh-Pt})$  (Fig. 2A). An experimentally-derived estimate of  $J_{\text{SQ-NN}}$  for the LL'CT excited state of **6-Me-*m*-Ph-Pt** is obtained from  $J_{\text{SQ-NN}}$  in the *ground state* biradical ligand of **LZnSQ-6-Me-*m*-Ph-NN** (Fig. 3). The **SQ-6-Me-*m*-Ph-NN** linkage in **LZnSQ-6-Me-*m*-Ph-NN** is, by analogy, the two-

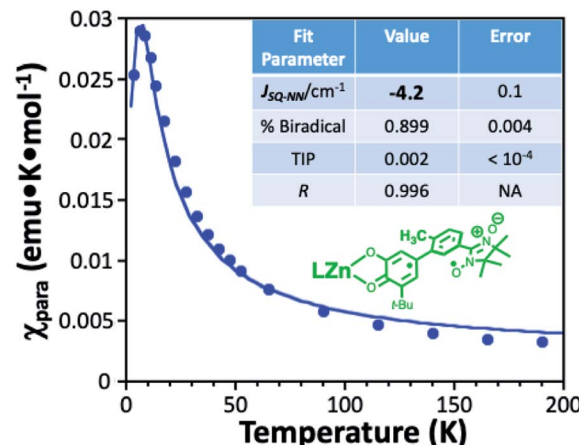


Fig. 3 Variable-temperature paramagnetic susceptibility data for **LZn(SQ-6-Me-*m*-Ph-NN)** (*L* = hydro-tris(cumanyl, methyl-pyrazolyl) borate), see ESI† for details. The best fit of eqn (2) to the data yields  $J_{\text{SQ-NN}} = -4\, \text{cm}^{-1}$ .

spin donor half of the charge separated LL'CT excited state for **6-Me-*m*-Ph-Pt**.

The magnitude of the antiferromagnetic  $J_{\text{SQ-NN}}$  mediated by an unsubstituted *m*-Ph bridge has previously been determined from solid state magnetic susceptibility measurements on **LZnSQ-*m*Ph-NN** ( $J_{\text{SQ-NN}} = -32\, \text{cm}^{-1}$ ).<sup>41</sup> The same Heisenberg-Dirac-Vleck spin Hamiltonian (eqn (1)) is used here to describe the exchange split singlet and triplet components of the **LZnSQ-6-Me-*m*-Ph-NN** ground state. The corresponding expression for the magnetic susceptibility is given by eqn (2), which is used to determine the singlet-triplet energy gap ( $\Delta_{\text{S-T}} = -2J_{\text{SQ-NN}}$ ) for **LZn(SQ-6-Me-*m*-Ph-NN)**. In eqn (2),  $x$  is percentage of the biradical that contributes to the susceptibility,  $(1 - x)$  is the mole fraction of the monoradical impurity, and TIP is the temperature-independent paramagnetism.<sup>42,43</sup>

$$\hat{H} = -2J_{\text{SQ-NN}} \hat{S}_1 \hat{S}_2 \quad (1)$$

$$\chi_{\text{para}} = x \frac{0.5 \text{ emu mol}^{-1}}{T} \left( \frac{\frac{2J_{\text{SQ-NN}}}{k_{\text{B}}T}}{1 + 3e^{\frac{2J_{\text{SQ-NN}}}{k_{\text{B}}T}}} \right) + (1 - x) 0.375 \text{ emu mol T}^{-1} + \text{TIP} \quad (2)$$

The  $\Delta_{\text{S-T}}$  value that we obtain by fitting eqn (2) to the magnetic susceptibility data (Fig. 3) for **LZn(SQ-6-Me-*m*-Ph-NN)** is  $\Delta_{\text{S-T}} = 8.0\, \text{cm}^{-1}$  ( $J_{\text{SQ-NN}} = -4.0\, \text{cm}^{-1}$ ), which corresponds to an 87% decrease in the magnetic exchange coupling relative to **LZn(SQ-*m*Ph-NN)**.<sup>10,44</sup> For conjugated systems, the attenuation of  $\pi$ -type superexchange coupling between SQ and NN is approximated by the product of the cosine squared of bond torsion angles for the SQ-bridge and bridge-NN linkages.<sup>10,44</sup> Based solely on the differences in SQ-bridge-NN torsion angles, this is expected to reduce the magnitude of  $J_{\text{SQ-NN}}$  for **LZn(SQ-6-Me-*m*-Ph-NN)** by >99% relative to **LZn(SQ-*m*Ph-NN)**. The larger experimental  $J_{\text{SQ-NN}}$  value observed for **LZn(SQ-6-Me-*m*-Ph-NN)**,



compared to that predicted solely by the bond torsion angles, derives from a combination of weak  $\sigma$ - and configuration interaction contributions to the exchange.<sup>10,41</sup> Critically, the bridge methyl group attenuates antiferromagnetic  $J_{\text{SQ-NN}}$  exchange in **LZn(SQ-6-Me-mPh-NN)** and this translates to a similar attenuation of  $J_{\text{SQ-NN}}$  in the LL'/CT excited state of **6-Me-mPh-Pt** that results in  $\Delta E_{\text{D}1\text{Q}}(\text{6-Me-mPh-Pt}) < \Delta E_{\text{D}1\text{Q}}(\text{mPh-Pt})$  (Fig. 2A).

## Excited state exchange determines ground state electron spin polarization

Low-temperature EPR and time-resolved EPR (TREPR) spectra of **mPh-Pt** and **6-Me-mPh-Pt** are presented in Fig. 4A and B, respectively, and these data highlight the dramatic difference in their spin polarized EPR signals at virtual parity of their molecular (but not conformational) structure, ground-state EPR spectra, and LL'/CT energy. Note that the direct-detection method used to measure the TREPR spectra is insensitive to static EPR signals and the difference between EPR absorbance before, and after, the laser flash is taken. Thus, a signal is only observed when time-dependent spin polarization is generated. We note that no ESP is generated in  $(\text{DMSO})_2\text{Pt}(\text{CAT-}m\text{-Ph-NN})$ , which lacks an LL'/CT excited state, indicating that the LL'/CT excited state is necessary to observe ground state ESP in these systems.<sup>16</sup>

Remarkably, and contrary to the predictions of the RQM, we observe *emissive* ESP in the recovered ground state of **6-Me-mPh-Pt** and *absorptive* ESP in the recovered ground state of **mPh-Pt**. Thus, the non-Boltzmann population distribution within the  $^2\text{S}_0$   $m_s = \pm 1/2$  sublevels generated by the laser-induced excitation/relaxation photocycle (Fig. 2A and 5) differs markedly for these two complexes. The differences in the nature of the ESP for **mPh-Pt** and **6-Me-mPh-Pt** correlate with the bridge-dependent energy gaps between  $^2\text{T}_1$  and the other states ( $^4\text{T}_1$ ,  $^2\text{NN}$ ,  $^4\text{NN}$ ) in this energy region, which are affected by CAT/SQ-

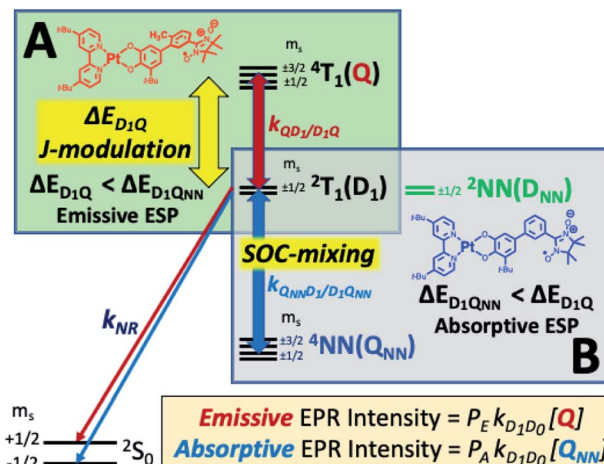


Fig. 5 (A) The reversed quartet mechanism (RQM). Mixing of chromophoric  $^2\text{T}_1$  and  $^4\text{T}_1$  states, mediated by conformational  $J_{\text{SQ-NN}}$ -modulation, gives rise to emissive ESP for **6-Me-mPh-Pt**. (B) Spin-orbit induced mixing of chromophoric  $^2\text{T}_1$  and the NN-based quartet state,  $^4\text{NN}$ , gives rise to absorptive ESP for **mPh-Pt**. The  $^2\text{NN}$  state can be observed spectroscopically (see ESI†).

bridge bond torsions. Since the degree of charge separation in the excited state manifolds of **mPh-Pt** and **6-Me-mPh-Pt** is near unity,<sup>13</sup> the  $J_{\text{SQ-NN}}$  value for **LZn(SQ-6-Me-mPh-NN)** can be used as a proxy for  $J_{\text{SQ-NN}}$  in the excited state of **6-Me-mPh-Pt**. The  $J_{\text{SQ-NN}}$  exchange interaction that we obtain for **LZn(SQ-6-Me-mPh-NN)** is related to the  $^2\text{T}_1$ – $^4\text{T}_1$  energy gap ( $\Delta E_{\text{D}1\text{Q}}$ ) in the three-spin excited states of **mPh-Pt** and **6-Me-mPh-Pt** according to  $\Delta E_{\text{D}1\text{Q}} = 1.5 J_{\text{SQ-NN}}$  when  $J_{\text{bpy-SQ}} \gg J_{\text{SQ-NN}}$ .<sup>17</sup> Thus, the  $^2\text{T}_1$ – $^4\text{T}_1$  energy gaps ( $\Delta E_{\text{D}1\text{Q}}$ ) are  $48 \text{ cm}^{-1}$  for **mPh-Pt** and  $6 \text{ cm}^{-1}$  for **6-Me-mPh-Pt**, respectively.

These  $\Delta E_{\text{D}1\text{Q}}$  values indicate that <6% of the **mPh-Pt**  $^4\text{T}_1$  state would be populated at thermal equilibrium at 20 K (the temperature at which the EPR spectra were recorded), but this increases dramatically to  $\sim 56\%$   $^4\text{T}_1$  population for **6-Me-mPh-Pt** at the same temperature. These populations are significant because the RQM (Fig. 1A and 4) requires thermal population of the  $^4\text{T}_1(\text{Q})$  state and spin-orbit coupling (SOC) induced zero-field mixing between the  $^2\text{T}_1$ – $^4\text{T}_1$  states to observe ground- and excited state ESP in **mPh-Pt** and **6-Me-mPh-Pt**. SOC induced interconversion rates between Zeeman split  $^2\text{T}_1$  and  $^4\text{T}_1$  states are given by the rate constants  $k_{\text{DQ}}$  and  $k_{\text{QD}}$  (Fig. 5), with  $k_{\text{DQ}}$  and  $k_{\text{QD}}$  being related by the equilibrium Boltzmann populations between the two levels (*i.e.*  $k_{\text{DQ}} = k_{\text{QD}} e^{-2J_{\text{SQ-NN}}/kT}$ ).<sup>35,36</sup> Given that  $J_{\text{SQ-NN}}$  is antiferromagnetic in **6-Me-mPh-Pt**, the RQM correctly predicts *emissive* ground state ESP due to  $E(^4\text{T}_1) > E(^2\text{T}_1)$ ,  $^2\text{T}_1$ – $^4\text{T}_1$  SOC state mixing, and  $k_{\text{QD}} > k_{\text{DQ}}$ .<sup>35,36</sup> Since **mPh-Pt** displays absorptive ground state ESP and a significantly larger  $^2\text{T}_1(\text{D}_1)$ – $^4\text{T}_1(\text{Q})$  energy gap, a different ESP mechanism must be operational for this complex.

Recently, we described how localized NN radical  $^2\text{NN}(\text{D}_{\text{NN}})$  and  $^4\text{NN}(\text{Q}_{\text{NN}})$  states (Fig. 4B) may be nearly isoenergetic with the  $^2\text{T}_1$  state of **mPh-Pt**.<sup>16</sup> We propose that the dynamic population of the  $^4\text{NN}$  state effectively competes with the higher energy  $^4\text{T}_1$  state to determine the sign of the ground state ESP. This competition is

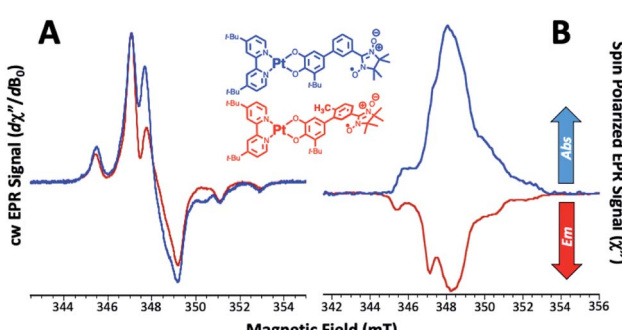


Fig. 4 X-band cw-EPR (A); 20 K; 2-MTHF, and TREPR (B); 20 K; 2-MTHF spectra for **mPh-Pt** (blue lines) and **6-Me-mPh-Pt** (red lines). (A) Field modulation detected cw-EPR spectra of the ground states without light excitation. (B) Light-induced, spin-polarized TREPR spectra, extracted from time/field datasets 4  $\mu\text{s}$  after the laser flash. Light excitation at 532 nm, concentrations  $\sim 0.5 \text{ mM}$ . Abs = absorption, Em = emission.



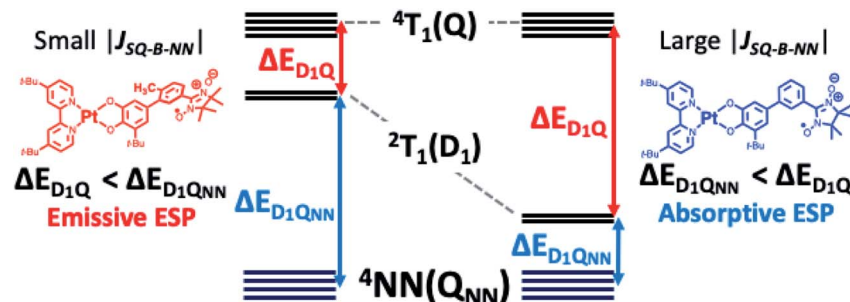


Fig. 6 Origins of emissive and absorptive ESP for NN-elaborated (bpy)Pt(CAT) complexes. Left: RQM with emissive ESP is observed. Right: RQM with absorptive ESP is observed.

readily apparent in **mPh-Pt** and results from the larger value of  $J_{SQ-NN}$  for this complex, which leads to a larger  $\Delta E_{D1Q}$  energy gap, a more stabilized  $^2T_1$  state, and  $\Delta E_{D1Q} > \Delta E_{D1QNN}$  between chromophoric  $^2T_1$  and  $Q_{NN}$  states (Fig. 5). The inclusion of additional states in the context of the RQM is key, as it correctly predicts the experimentally observed *absorptive* ESP via  $^2T_1 \leftrightarrow Q_{NN}$  mixing for **mPh-Pt**. Thus, the magnitude of the antiferromagnetic excited state exchange interaction,  $J_{SQ-NN}$ , controls how the  $^2T_1$  state mixes with neighboring excited states to switch the *sign* of the ground state ESP. This observation highlights the effectiveness of TREPR spectroscopy for revealing details of fast non-radiative processes that are difficult to detect using other spectroscopic methods. In the present case, the sign of the ground state ESP reveals how the small energy gap between charge transfer and localized excited states, coupled with the relative magnitudes of interstate mixing, critically alters the spin selectivity of the electronic relaxation.

## Conclusions

In summary, we observe dramatic differences in ground state ESP for **mPh-Pt** and **6-Me-mPh-Pt** that are attributed to the energies of their  $^2T_1$  states relative to chromophoric  $^4T_1(Q)$  states and a localized radical-based  $Q_{NN}$  state (Fig. 6). For **6-Me-mPh-Pt**, an LL/CT excited state SQ-bridge bond torsion effectively attenuates the magnitude of the excited state  $J_{SQ-NN}$  antiferromagnetic exchange interaction, which leads to  $\Delta E_{D1Q} < \Delta E_{D1QNN}$  and emissive ESP as described by the RQM (Fig. 1A) and observed experimentally (Fig. 4B). Conversely, the comparatively planar CAT-*mPh-NN*  $\pi$ -system of **mPh-Pt** results in  $\Delta E_{D1QNN} < \Delta E_{D1Q}$ , and absorptive ESP is both predicted and observed (Fig. 1B and 4B, respectively). Thus, small conformational changes along low-frequency torsional modes of donor-acceptor molecules that have been elaborated with pendant persistent radicals can lead to conformational  $J$ -modulation, and this affects the sign and magnitude of the ground state ESP. This indicates that the sign of the excited state chromophore-radical exchange predicted by the RQM is not universal, and our work points to a previously unobserved change in ground state ESP as a function of the *magnitude* of the excited state exchange interaction,  $J_{SQ-NN}$ . The present results highlight the extreme importance of understanding how excited state electronic structure affects excited state properties and dynamics,

and demonstrates additional mechanisms to control ESP relevant to QIS. Ongoing research efforts focus on further exploration of synthetic design principles directed toward determining the electronic and geometric structure factors that control optically-generated ESP in these and related radical-elaborated donor-acceptor chromophores, and how these can be exploited for QIS applications.

## Experimental

### General considerations

Reagents and solvents were used as received and purchased from commercial vendors. See ESI† for compound syntheses and characterization.

### Magnetic susceptibility measurements

Magnetic susceptibility measurements were collected on a Quantum Design MPMS-XL7 SQUID magnetometer. Variable temperature magnetometry experiments were performed with a constant field of 0.7 T on a microcrystalline sample ( $\sim 15$  mg) which was loaded into a gelcap/straw sample holder and mounted to the sample rod with Kapton tape. Collected raw data was initially corrected with a straight line for diamagnetic response of sample and container as a first approximation, where the slope of the line represents the residual diamagnetic correction.

### EPR and TREPR spectroscopies

Samples for steady state and transient EPR measurements were prepared by dissolving solid (bpy)Pt(CAT-*mPh-NN*), (**mPh-Pt**) or (bpy)Pt(CAT-*6-Me-mPh-NN*), (**6-Me-mPh-Pt**) in 2-methylTHF to a concentration of  $\sim 0.5$  mM. The samples were placed in 4 mm O.D. quartz EPR tubes and degassed by repeated freeze-pump-thaw cycles. The frozen, degassed samples were then transferred without thawing from liquid nitrogen to the spectrometer cryostat, which was at 20 K. The steady state spectra were collected using field modulation detection with a modulation amplitude of 0.1 mT and a microwave power of 6.3 mW. TREPR time/field dataset were collected with direct detection at the microwave power as for the steady state experiments. The samples were irradiated at 532 nm using 10 ns laser flashes from a frequency doubled NdYAG laser. The modified Bruker EPR 200D-SRC X-band spectrometer used for the EPR experiments has been described in detail elsewhere.<sup>45</sup>



## Data availability

The datasets supporting this article have been uploaded as part of the ESI.†

## Author contributions

M. L. K. supervised the research, vetted the data, and wrote the manuscript. D. A. S. supervised the research, vetted the data, and wrote the manuscript. P. H. synthesized and characterized the compounds. D. E. S. synthesized and characterized the compounds. J. C. performed electronic structure computations. A. v. d. E. supervised the research, vetted the data, and wrote the manuscript.

## Conflicts of interest

No competing financial interests have been declared.

## Acknowledgements

M. L. K. and D. A. S. acknowledge financial support from DOE (DE-SC0020199). A. v. d. E. acknowledges support from NSERC (Discovery grant 2015-04021).

## References

- 1 M. R. Wasielewski, M. D. E. Forbes, N. L. Frank, K. Kowalski, G. D. Scholes, J. Yuen-Zhou, M. A. Baldo, D. E. Freedman, R. H. Goldsmith, T. Goodson, M. L. Kirk, J. K. McCusker, J. P. Ogilvie, D. A. Shultz, S. Stoll and K. B. Whaley, Exploiting chemistry and molecular systems for quantum information science, *Nat. Rev. Chem.*, 2020, **4**(9), 490–504.
- 2 J. Lehmann, A. Gaita-Arino, E. Coronado and D. Loss, Quantum computing with molecular spin systems, *J. Math. Chem.*, 2009, **19**(12), 1672–1677.
- 3 A. Palii, S. Aldoshin and B. Tsukerblat, Mixed-Valence Triferrocenium Complex with Electric Field Controllable Superexchange as a Molecular Implementation of Triple Quantum Dot, *J. Phys. Chem. C*, 2017, **121**(48), 27218–27224.
- 4 P. C. E. Stamp and A. Gaita-Arino, Spin-based quantum computers made by chemistry: hows and whys, *J. Math. Chem.*, 2009, **19**(12), 1718–1730.
- 5 D. P. DiVincenzo, The physical implementation of quantum computation, *Fortschr. Phys.*, 2000, **48**(9–11), 771–783.
- 6 K. S. Akhilesh, B. G. Divyamani, Sudha, A. R. U. Devi and K. S. Mallesh, Spin squeezing in symmetric multiqubit states with two non-orthogonal Majorana spinors, *Quantum Inf. Process.*, 2019, **18**(5), 144.
- 7 V. A. Soltamov, C. Kasper, A. V. Poshakinskiy, A. N. Anisimov, E. N. Mokhov, A. Sperlich, S. A. Tarasenko, P. G. Baranov, G. V. Astakhov and V. Dyakonov, Excitation and coherent control of spin qudit modes in silicon carbide at room temperature, *Nat. Commun.*, 2019, **10**, 1678.
- 8 A. de, A. Lang, D. Zhou and R. Joynt, Suppression of decoherence and disentanglement by the exchange interaction, *Phys. Rev.*, 2011, **83**(4), 042331.
- 9 M. Orrit, Molecular Entanglements, *Science*, 2002, **298**(5592), 369.
- 10 D. A. Shultz, M. L. Kirk, J. Y. Zhang, D. E. Stasiw, G. B. Wang, J. Yang, D. Habel-Rodriguez, B. W. Stein and R. D. Sommer, Spectroscopic Signatures of Resonance Inhibition Reveal Differences in Donor-Bridge and Bridge-Acceptor Couplings, *J. Am. Chem. Soc.*, 2020, **142**(10), 4916–4924.
- 11 C. R. Tichnell, D. R. Daley, B. W. Stein, D. A. Shultz, M. L. Kirk and E. O. Danilov, Wave Function Control of Charge-Separated Excited-State Lifetimes, *J. Am. Chem. Soc.*, 2019, **141**(9), 3986–3992.
- 12 B. W. Stein, D. A. Dickie, S. Nedungadi, D. J. R. Brook, D. A. Shultz and M. L. Kirk, Long-range spin dependent delocalization promoted by the pseudo Jahn-Teller effect, *J. Chem. Phys.*, 2019, **151**(20), 201103.
- 13 J. Yang, D. K. Kersi, C. P. Richers, L. J. Giles, R. Dangi, B. W. Stein, C. Feng, C. R. Tichnell, D. A. Shultz and M. L. Kirk, Ground State Nuclear Magnetic Resonance Chemical Shifts Predict Charge-Separated Excited State Lifetimes, *Inorg. Chem.*, 2018, **57**(21), 13470–13476.
- 14 D. E. Stasiw, J. Y. Zhang, G. B. Wang, R. Dangi, B. W. Stein, D. A. Shultz, M. L. Kirk, L. Wojtas and R. D. Sommer, Determining the Conformational Landscape of  $\sigma$  and  $\pi$  Coupling Using para-Phenylenes and "Aviram-Ratner" Bridges, *J. Am. Chem. Soc.*, 2015, **137**(29), 9222–9225.
- 15 J. Yang, D. K. Kersi, L. J. Giles, B. W. Stein, C. J. Feng, C. R. Tichnell, D. A. Shultz and M. L. Kirk, Ligand Control of Donor-Acceptor Excited-State Lifetimes, *Inorg. Chem.*, 2014, **53**(10), 4791–4793.
- 16 M. L. Kirk, D. A. Shultz, J. Chen, P. Hewitt, D. Daley, S. Paudel and A. van der Est, Metal Ion Control of Photoinduced Electron Spin Polarization in Electronic Ground States, *J. Am. Chem. Soc.*, 2021, **143**(28), 10519–10523.
- 17 B. W. Stein, C. R. Tichnell, J. Chen, D. A. Shultz and M. L. Kirk, Excited State Magnetic Exchange Interactions Enable Large Spin Polarization Effects, *J. Am. Chem. Soc.*, 2018, **140**(6), 2221–2228.
- 18 M. Milivojevic, Maximal thermal entanglement using three-spin interactions, *Quantum Inf. Process.*, 2019, **18**(2), 1–14.
- 19 Z. B. Zheng Yi-Dan, Tripartite entanglement of  $\{\text{Cu}_3\}$  single molecular magnet with magnetic field in thermal equilibrium, *Acta Phys. Sin.*, 2016, **65**(12), 120301.
- 20 P. Amit Kumar and B. Indrani, Entanglement in a molecular three-qubit system, *J. Phys.: Condens. Matter*, 2010, **22**(1), 016004.
- 21 Z. J. Wang, Y. T. Gao, M. Hussain, S. Kundu, V. Rane, M. Hayvali, E. A. Yildiz, J. Z. Zhao, H. G. Yaglioglu, R. Das, L. Luo and J. F. Li, Efficient Radical-Enhanced Intersystem Crossing in an NDI-TEMPO Dyad: Photophysics, Electron Spin Polarization, and Application in Photodynamic Therapy, *Chem.- Eur. J.*, 2018, **24**(70), 18663–18675.
- 22 A. Ito, A. Shimizu, N. Kishida, Y. Kawanaka, D. Kosumi, H. Hashimoto and Y. Teki, Excited-State Dynamics of Pentacene Derivatives with Stable Radical Substituents, *Angew. Chem., Int. Ed.*, 2014, **53**(26), 6715–6719.
- 23 Y. Teki and T. Matsumoto, Theoretical study of dynamic electron-spin-polarization via the doublet-quartet



quantum-mixed state and time-resolved ESR spectra of the quartet high-spin state, *Phys. Chem. Chem. Phys.*, 2011, **13**(13), 5728–5746.

24 M. T. Colvin, E. M. Giacobbe, B. Cohen, T. Miura, A. M. Scott and M. R. Wasielewski, Competitive Electron Transfer and Enhanced Intersystem Crossing in Photoexcited Covalent TEMPO-Perylene-3,4:9,10-bis(dicarboximide) Dyads: Unusual Spin Polarization Resulting from the Radical-Triplet Interaction, *J. Phys. Chem. A*, 2010, **114**(4), 1741–1748.

25 Y. Teki and T. Matsumoto, Spin dynamics on photoexcited state of functionality  $\pi$ -radical via quantum-mixed state: Theoretical study of the spin polarized state generation using the mechanism via quantum-mixed state, *Synth. Met.*, 2013, **173**, 35–39.

26 T. Matsumoto and Y. Teki, Theoretical study of dynamic electron-spin-polarization via the doublet-quartet quantum-mixed state (II). Population transfer and magnetic field dependence of the spin polarization, *Phys. Chem. Chem. Phys.*, 2012, **14**(29), 10178–10186.

27 M. Zarea, M. A. Ratner and M. R. Wasielewski, Spin polarization transfer by the radical pair mechanism, *J. Chem. Phys.*, 2015, **143**(5), 054101.

28 E. T. Chernick, R. Casillas, J. Zirzlmeier, D. M. Gardner, M. Gruber, H. Kropp, K. Meyer, M. R. Wasielewski, D. M. Guldi and R. R. Tykwiński, Pentacene Appended to a TEMPO Stable Free Radical: The Effect of Magnetic Exchange Coupling on Photoexcited Pentacene, *J. Am. Chem. Soc.*, 2015, **137**(2), 857–863.

29 M. T. Colvin, R. Carmieli, T. Miura, S. Richert, D. M. Gardner, A. L. Smeigh, S. M. Dyar, S. M. Conron, M. A. Ratner and M. R. Wasielewski, Electron Spin Polarization Transfer from Photogenerated Spin-Correlated Radical Pairs to a Stable Radical Observer Spin, *J. Phys. Chem. A*, 2013, **117**(25), 5314–5325.

30 Q. X. Mi, E. T. Chernick, D. W. McCamant, E. A. Weiss, M. A. Ratner and M. R. Wasielewski, Spin dynamics of photogenerated triradicals in fixed distance electron donor-chromophore-acceptor-TEMPO molecules, *J. Phys. Chem. A*, 2006, **110**(23), 7323–7333.

31 E. T. Chernick, Q. X. Mi, R. F. Kelley, E. A. Weiss, B. A. Jones, T. J. Marks, M. A. Ratner and M. R. Wasielewski, Electron donor-bridge-acceptor molecules with bridging nitronyl nitroxide radicals: Influence of a third spin on charge- and spin-transfer dynamics, *J. Am. Chem. Soc.*, 2006, **128**(13), 4356–4364.

32 Y. E. Kand rashkin and A. van der Est, The triplet mechanism of electron spin polarization in moderately coupled triplet-doublet rigid complexes as a source of the enhanced  $+1/2 \leftrightarrow -1/2$  transitions, *J. Chem. Phys.*, 2019, **151**, 184301.

33 Y. E. Kand rashkin and A. van der Est, Orientation Information from the Dipolar Interaction Between a Complex in the Excited Quartet State and a Doublet Spin Label, *Appl. Magn. Reson.*, 2014, **45**(3), 217–237.

34 Y. Kand rashkin and A. van der Est, Electron spin polarization of the excited quartet state of strongly coupled triplet-doublet spin systems, *J. Chem. Phys.*, 2004, **120**, 4790–4799.

35 V. Rozenshtein, A. Berg, E. Stavitski, H. Levanon, L. Franco and C. Corvaja, Electron spin polarization of functionalized fullerenes. Reversed quartet mechanism, *J. Phys. Chem. A*, 2005, **109**(49), 11144–11154.

36 A. K. Tripathi, V. Rane, S. Kundu and R. Das, A phenomenological scheme for reversed quartet mechanism of electron spin polarization in covalently linked systems of chromophore and free radical: Determination of magnitude of polarization and application to pyrene-TEMPO linked molecules, *J. Chem. Phys.*, 2019, **151**(15), 154305.

37 K. Ishii, Y. Hirose, H. Fujitsuka, O. Ito and N. Kobayashi, Time-resolved EPR, fluorescence, and transient absorption studies on phthalocyaninatosilicon covalently linked to one or two TEMPO radicals, *J. Am. Chem. Soc.*, 2001, **123**(4), 702–708.

38 K. Kanemoto, A. Fukunaga, M. Yasui, D. Kosumi, H. Hashimoto, H. Tamekuni, Y. Kawahara, Y. Takemoto, J. Takeuchi, Y. Miura and Y. Teki, Ultrafast photoexcitation dynamics of  $\pi$ -conjugated bipy-anthracene-radical triad system, *RSC Adv.*, 2012, **2**(12), 5150–5153.

39 M. L. Kirk, D. A. Shultz, E. C. Depperman and C. L. Brannen, Donor-acceptor biradicals as ground state analogues of photoinduced charge separated states, *J. Am. Chem. Soc.*, 2007, **129**(7), 1937–1943.

40 G. Bussiere, R. Beaulac, H. Belisle, C. Lescop, D. Luneau, P. Rey and C. Reber, Excited states and optical spectroscopy of nitronyl nitroxides and their lanthanide and transition metal complexes, in *Transition Metal and Rare Earth Compounds III: Excited States, Transitions, Interactions*, ed. H. Yersin, 2004, vol. 241, pp. 97–.

41 M. L. Kirk, D. A. Shultz, D. E. Stasiw, D. Habel-Rodriguez, B. Stein and P. D. Boyle, Electronic and Exchange Coupling in a Cross-Conjugated D-B-A Biradical: Mechanistic Implications for Quantum Interference Effects, *J. Am. Chem. Soc.*, 2013, **135**(39), 14713–14725.

42 E. A. Boudreux and L. N. Mulay, *Theory and applications of molecular paramagnetism*, Wiley Interscience, New York, 1976, p. 510.

43 O. Kahn, *Molecular Magnetism*, VCH, New York, 1993, p. 380.

44 D. E. Stasiw, J. Y. Zhang, G. B. Wang, R. Dangi, B. W. Stein, D. A. Shultz, M. L. Kirk, L. Wojtas and R. D. Sommer, Determining the Conformational Landscape of  $\sigma$  and  $\pi$  Coupling Using para-Phenylenes and “Aviram-Ratner” Bridges, *J. Am. Chem. Soc.*, 2015, **137**(29), 9222–9225.

45 W. Xu, P. Chitnis, A. Valieva, A. van der Est, Y. N. Pushkar, M. Krzstyniak, C. Teutloff, S. G. Zech, R. Bittl, D. Stehlík, B. Zyballov, G. Z. Shen and J. H. Golbeck, Electron transfer in cyanobacterial photosystem I - I. Physiological and spectroscopic characterization of site-directed mutants in a putative electron transfer pathway from A(0) through A(1) to F-x, *J. Biol. Chem.*, 2003, **278**(30), 27864–27875.

